

EXPERIMENTAL BUCKLING TESTS AND NUMERICAL ANALYSES OF STIFFENED CYLINDRICAL SHELLS IN COMPOSITE MATERIALS

Chiara Bisagni, Potito Cordisco and Luca Lanzi
 Dipartimento di Ingegneria Aerospaziale, Politecnico di Milano
 Via La Masa 34, 20156 Milano, Italy, E-mail: Chiara.Bisagni@polimi.it

Keywords: *Buckling, composite stiffened shells, experimental tests*

Abstract

The work presented in this paper is part of a larger research project aiming at improving the knowledge of the buckling behaviour of composite stiffened shell structures. In particular, it investigates experimentally and numerically the buckling and post-buckling phenomena of CFRP stiffened thin-walled cylindrical shells.

The examined cylindrical shells, manufactured and provided by AGUSTA, are designed to work in the post-buckling field. Indeed, they present a first local buckling, limited to the cylinder skin and later a global buckling, that corresponds to the collapse load and involves the whole cylinder. The ratio between the collapse load and the local buckling load is about 4.

The experimental tests are performed under axial compression. An equipment allows to measure, by five laser displacement sensors, both the initial geometric imperfections and the buckling pattern development on the specimens internal surfaces during the tests.

The experimental results are then compared to those numerically obtained using the finite element code LS-DYNA. A slow dynamic analysis was used to obtain the load-displacement curve and to follow the post-buckling pattern.

1 Introduction

Aeronautical shells are mainly thin-walled structures, which can be subject to buckling under certain load cases [1]. As long as these

shells had been made of aluminium sheet metal, the consequences of buckling are well studied and generally covered by accepted methods of strength verification.

Nowadays, more and more effort is related to the implementation of composite shells, as result of weight optimization or for manufacturing reasons. Advanced composite materials have been investigated in-depth to allow a significant reduction in structural weight [2, 3, 4]. In particular carbon fiber reinforced plastic (CFRP) stiffened structures exhibits a great advantage in terms of their high strength-to-weight ratio over those constructed from metallic materials.

Besides, experiments have shown that the potential exists for further weight savings with stiffened composite structures by allowing post-buckling of the skin to occur during operation [5, 6, 7]. Where the skin of the structure is not too thick, it is well known that the buckling load does not represent the maximum load that the structure can carry.

Proper design enables to work in the post-buckled regime without any damage. This requires the acquisition of reliable data on material and structural behaviour beyond primary buckling and the development of appropriate simulation procedures and design guidelines.

The work presented in this paper is part of a larger research project, "POSICOSS – Improved Post-buckling Simulation for Design of Fibre Composite Stiffened Fuselage Structures", supported by the European Commission in the Fifth Framework, aiming at improving the

knowledge of the buckling and post-buckling behaviour of composite stiffened shell structures.

In particular, the paper presents experimental and numerical results of buckling and post-buckling phenomena of CFRP stiffened thin-walled cylindrical shells. The examined cylindrical shells, manufactured and provided by AGUSTA, present different number of L-shaped stiffeners and different types of lay-up orientation for the skin and the stiffeners. These stiffened shells are designed to work in the post-buckling field. Indeed, they present a first local buckling, limited to the cylinder skin, that remains so in the post-buckling field. Later a global buckling, that corresponds to the collapse load, involves the whole cylinder.

2 Cylindrical Stiffened Shells

Cylindrical stiffened shells with different number of L-shaped stiffeners and different types of lay-up orientation for the skin and the stiffeners are under investigation. They are characterised by a length and an internal diameter of 700 mm and they present two reinforced tabs at the top and bottom to allow to fix the specimens into the loading rig. The free length is therefore limited to the central part and is equal to 525 mm.

Here the results of cylindrical stiffened shells characterised by 8 L-shaped stiffeners (Figures 1 and 2) are presented.

The stiffener blades are 25 mm long while the parts in contact with the skin are 32 mm long. The stiffeners, equally spaced and equally oriented, have a rounded corner with a mean radius of 7 mm due to manufacture process and present a symmetric lay-up for 12 plies in total: $[0^\circ/90^\circ]_{3S}$. The stiffeners are bonded to the skin, and some rivets are added just for safety in case of debonding.

The cylinder skin consists of two plies, 0.33 mm thick, at $+45^\circ$ and -45° . Reinforced skin areas, 40 mm long, are obtained in correspondence of the stiffeners adding three layers outer the skin, so to obtain a lay-up in those areas equal to $[45^\circ/-45^\circ/0^\circ/-45^\circ/45^\circ]$.

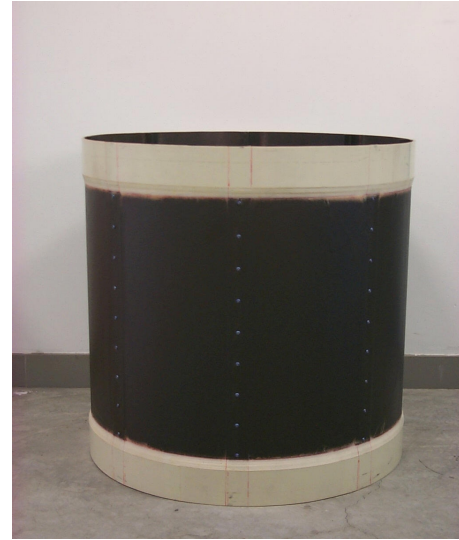


Fig. 1. A stiffened cylinder.



Fig. 2. Top view of a stiffened cylinder.

3 Experimental Equipment

A photo of the experimental equipment used to perform buckling tests with a position control mode is reported in Figure 3 [8].

To perform axial compression tests, the axial force is applied by a hydraulic ram against four adjustable ball screws, placed at the four corners of the platform. At the beginning, the load given by the ram is completely supported by the four screws, which distribute the real applied load on the specimen during the test. Indeed, the screws motion is computer-controlled, producing exactly the desired displacement to the loading platform, by means of four stepping motors through four reduction gears. Thus the load level, which is transferred smoothly to the cylinder, depends only on the platform displacement and on the cylinder

EXPERIMENTAL BUCKLING TESTS AND NUMERICAL ANALYSES OF STIFFENED CYLINDRICAL SHELLS IN COMPOSITE MATERIALS

elastic response and it does not substantially depend on the load magnitude due to the hydraulic ram acting on the platform.

The compression load is measured, during the tests, by means of a load cell situated under the lower clamp, while three LVDT transducers measure the axial displacement of the specimen in three equally spaced points. So it is possible to obtain the diagram of the compression load versus the axial displacement, during the tests.

The equipment allows to perform also buckling tests under torsion and under combined axial and torsion loading. To perform torsion tests, the rotation is given to the specimen bottom by means of a torsion lever, computer-controlled, like in the case of axial compression. The load cell, situated under the lower clamp, is able to measure also the torsion, while three LVDT transducers measure the tangential displacement of the specimen bottom. To perform buckling tests under combined axial and torsion loading, three different procedures can be applied: twisting the specimen to a pre-set torsion torque level and then in axially loading it until buckling; axially loading the specimen to a pre-set axial load level and then twisting it until buckling and a little further in post-buckling or applying fixed steps of axial load and torsion torque with different ratio of axial load and torsion torque levels.

An ad-hoc equipment (Figure 4) allows then to measure, on the specimens internal surface, the pre-buckling shape and the evolution of the post-buckling mode. The equipment is placed inside the specimen during the tests and employs five laser displacement sensors to measure the internal surface, so to avoid any contact with the specimen and consequently not to influence the buckling behaviour. The five laser displacement sensors are fixed on a slide, capable of rotating and vertically translating. The combination of the two movements allows to measure the internal surface of the specimens. These movements are generated by two stepping motors and the vertical position of the slide is determined by an incremental encoder. The laser displacement sensors are placed at the distance of 40 mm from the specimen internal surface. They guarantee a

measurement range of ± 10 mm with a resolution of 15 μm , for recording both the geometric imperfections (some tens of micrometers) and the post-buckling mode (about 10 - 20 mm). Normally the surface is measured 20-30 times during each test. The time required to measure a complete surface is limited to 4 minutes. The measurements are recorded in a regular grid of points 10 mm spaced both circumferentially and axially.



Fig. 3. Equipment for the buckling tests.



Fig. 4. Equipment for the measurement of the post-buckling mode.

4 Experimental Results

At first, different tests have been performed under axial compression until the local buckling. The tests have presented a repetitive behaviour. The local buckling loads obtained in the different tests are reported in Table 1.

Test number	Local buckling load [kN]
1	77.25
2	78.64
3	83.29
4	73.00

Table 1. Measured local buckling loads

Then a test until collapse has been performed under axial compression. Figure 5 reports the obtained load-displacement curve, while a photo taken during the test is reported in Figure 6. In the photo, the waves are clearly visible only in the lighted area, but they are present in all the cylinder.

Figures 7-12 report some of the internal surfaces measured by the laser sensors during the test. The points, where the internal surface has been measured, are reported on the load-displacement curve of Figure 5.

From the different Figures, it is possible to see that the cylinder deformation started with a local buckling at 85 kN, limited to the cylinder skin. The deformation developed with small waves near the upper and lower edges of the shells. Then the waves propagated in all the eight sectors between the stiffeners. At a load of about 130 kN there were two small waves in six sectors and just one bigger wave in two opposite sectors. Increasing the axial load, another small wave was born in almost each sector, centrally along the length and next to the stiffener. The three waves evolved around 230 kN forming a biggest central wave that presented internal and external displacements of about 16 mm and 14 mm, respectively. Then another big wave developed in almost all the sectors.

The collapse happened at a load equal to 312 kN, with an axial shortening of the cylinder equal to 3.33 mm. The collapse was due to the contemporary global buckling of 5 stiffeners. The ratio between the collapse load and the local buckling load was equal to about 4.

Figure 13 reports a photo of a failed stiffener.

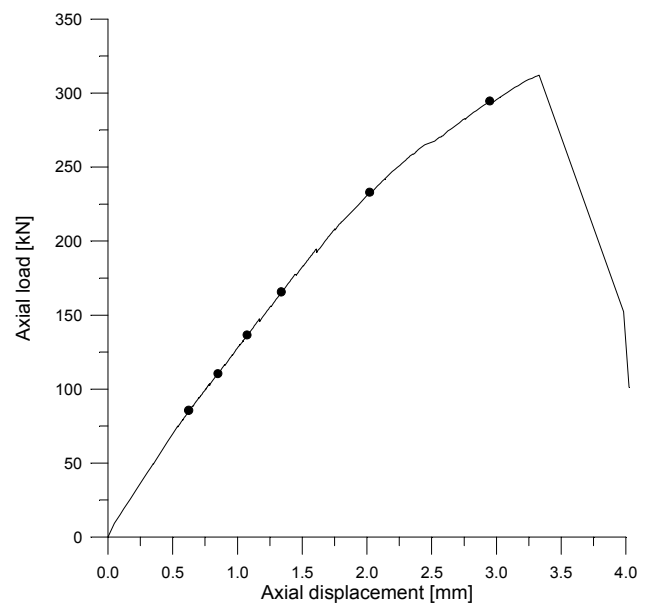


Fig. 5. Load-displacement curve.

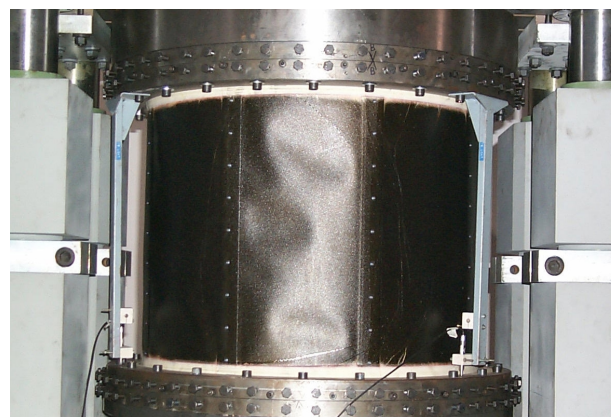


Fig. 6. Photo during the test.

EXPERIMENTAL BUCKLING TESTS AND NUMERICAL ANALYSES OF STIFFENED CYLINDRICAL SHELLS IN COMPOSITE MATERIALS

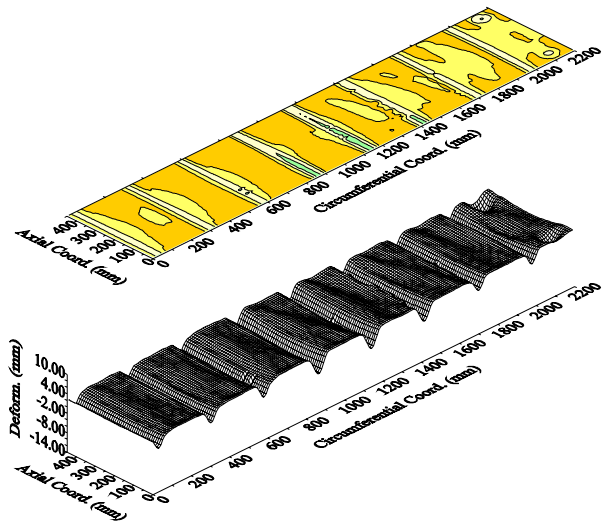


Fig. 7. Axial load = 85 kN.

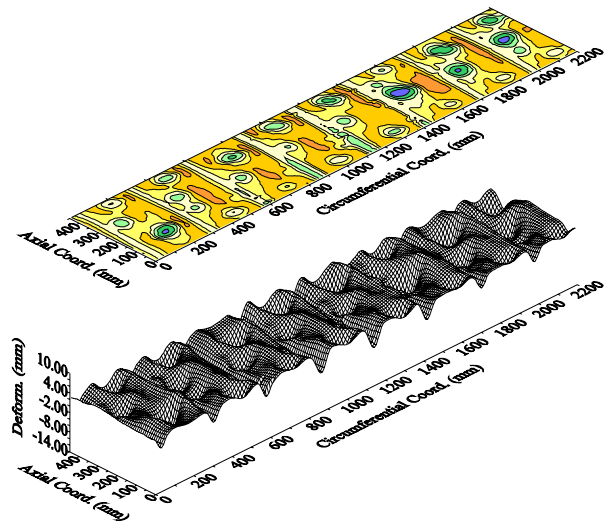


Fig. 10. Axial load = 165 kN.

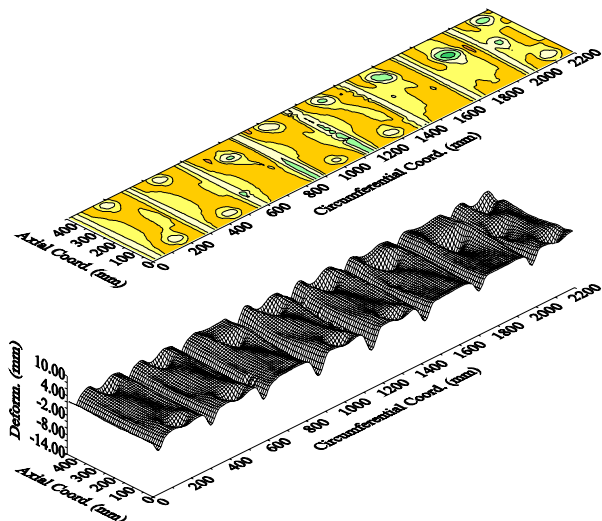


Fig. 8. Axial load = 110 kN.

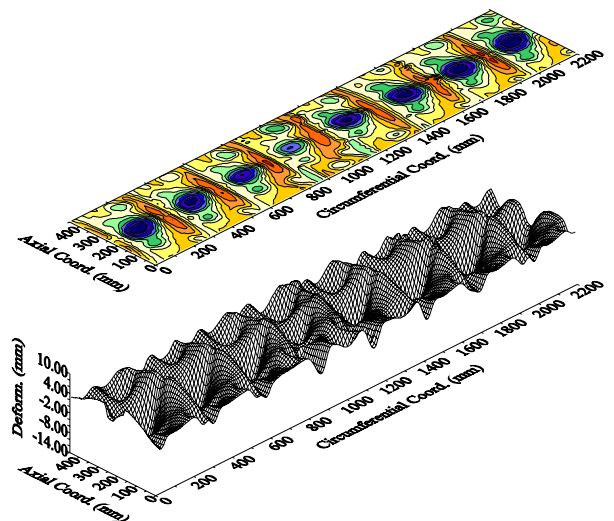


Fig. 11. Axial load = 233 kN.

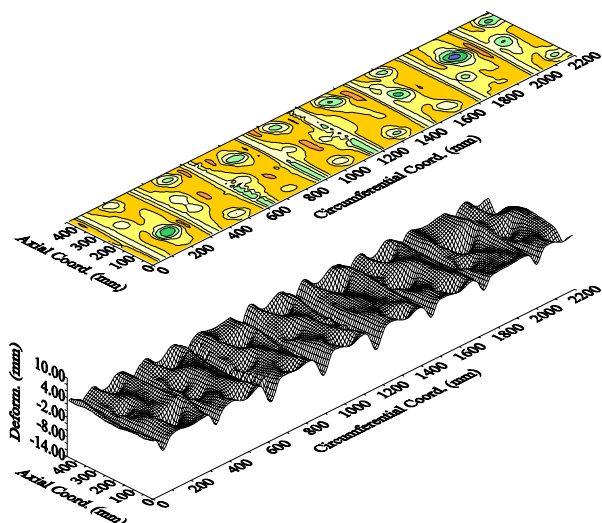


Fig. 9. Axial load = 136 kN.

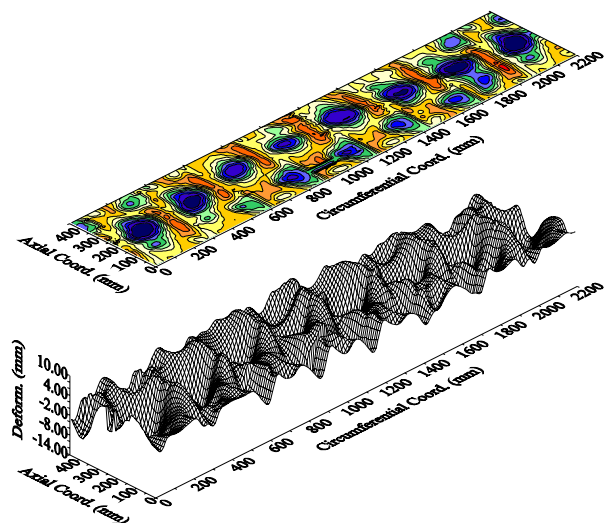


Fig. 12. Axial load = 294 kN.



Fig. 13. Photo of the failure of a stiffener.

5 Numerical Analyses

Finite element models [9] have been studied, having the same properties as the real stiffened shells, to be able to reproduce the results of the experimental tests, i.e. both the buckling load values and the post-buckling behaviour [10].

In the present study, the results obtained using the finite element code LS-DYNA [11] are presented. The analysis allows for the investigation of the load-displacement curve, including the post-buckling region, simulating the dynamics of a slow axial compression test.

The stiffened shells are modelled using 4-nodes bilinear shell elements. The finite element model's length is taken to be 525 mm, without the two reinforced tabs. The other geometric dimensions are the same as for the real shells. The upper and lower ends of the numerical models are constrained to remain plane and circular, maintaining the initial radius.

After performing mesh convergence studies, a mesh of 19832 shell elements (Hughes-Liu formulation) is used, so that the elements dimensions are about 8 x 8 mm, both in the skin and in the stiffeners.

The material model used is MAT 58, MAT-LAMINATED-COMPOSITE-FABRIC, as

implemented in LS-DYNA [11]. It allows to define a progressive damage model for composite fabrics. In particular, when the strength values are reached then the damage evolves in tension and compression for both the normal and transverse direction. The damage evolution is independent of any of the other stresses. A coupling is only present via the elastic material parameters and the complete structure behaviour. Non-linear shear behaviour is also considered defining a curve of shear stress versus shear strain.

The material properties introduced in the numerical model are tuned through numerical simulations of the material characterisation tests, performed until failure, according to the IEPG-CTP-TA 21 guidelines [12]. In this way, also the damage variables and the non-linear shear behaviour have been introduced into the model.

6 Numerical Results

Figure 14 reports the comparison of the load-displacement curve obtained numerically and experimentally.

The numerical evolution of the deformation in the post-buckling regime is presented in Figures 15-20, with a displacement scale factor equal to 3.

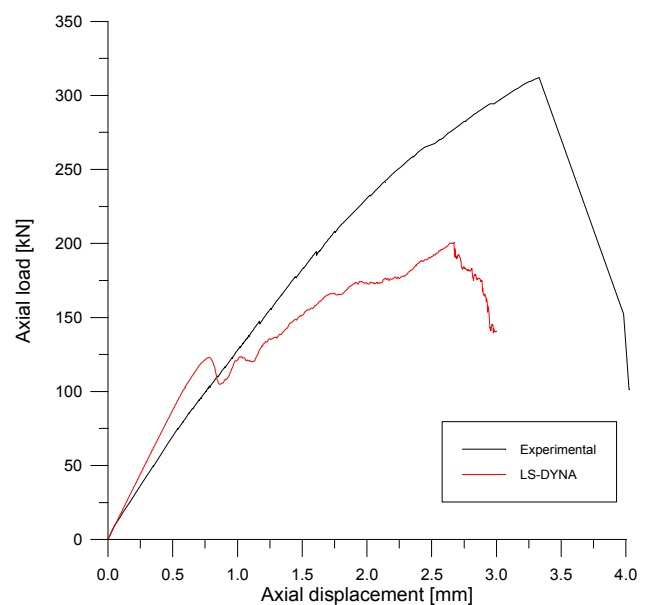


Fig. 14. Comparison between the experimental and the numerical load-displacement curves.

EXPERIMENTAL BUCKLING TESTS AND NUMERICAL ANALYSES OF STIFFENED CYLINDRICAL SHELLS IN COMPOSITE MATERIALS

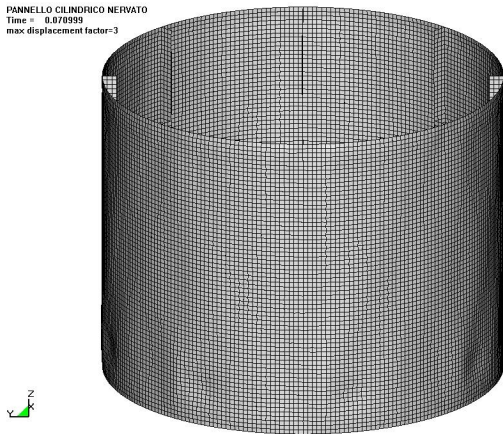


Fig. 15. Axial load = 118 kN.

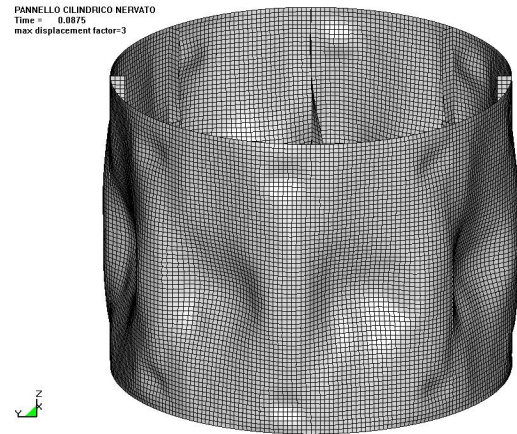


Fig. 18. Axial load = 151 kN.

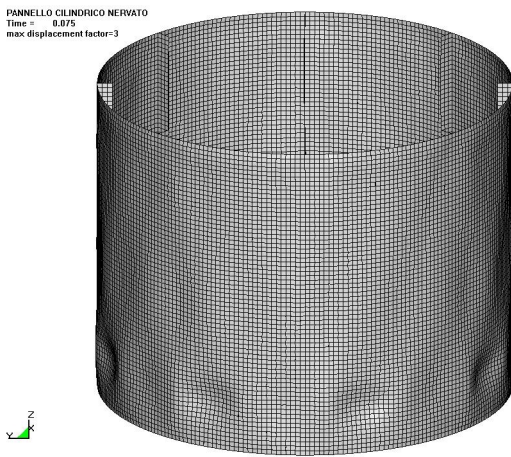


Fig. 16. Axial load = 121 kN.

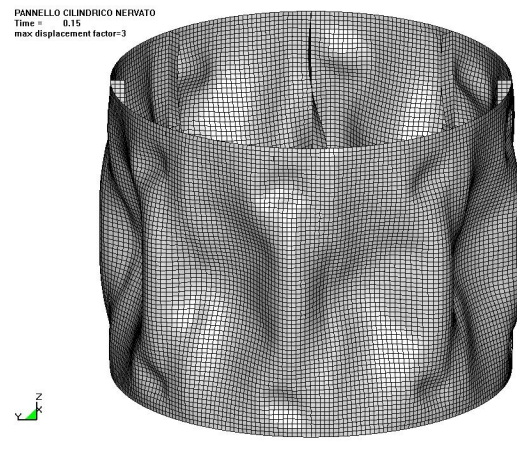


Fig. 19. Axial load = 174 kN.

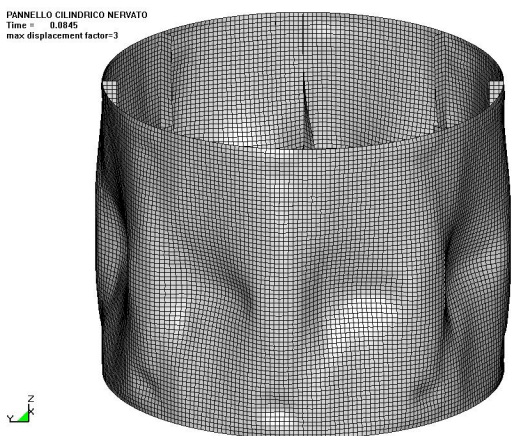


Fig. 17. Axial load = 133 kN.

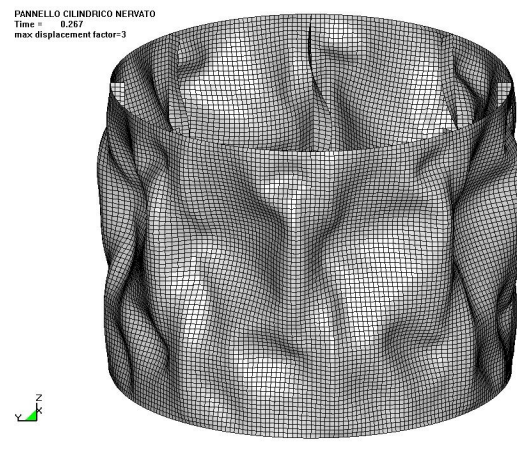


Fig. 20. Axial load = 204 kN.

It is possible to see that the local buckling load obtained with the LS-DYNA model is higher than the experimental value. Indeed, it is equal to 118 *kN*, while the experimental one is equal to about 85 *kN*. This can be due to the fact that in the numerical model neither the initial geometrical imperfections nor the thickness variations are yet included. Instead the numerical global buckling is equal to 205 *kN* compared to the experimental value equal to 312 *kN*, so it is significantly lower. This is probably due to how the LS-DYNA code introduces the damage model that is too penalising and conservative. Indeed, the prediction of the collapse load is very difficult because of the susceptibility of composites to the effect of the stress through the thickness. There are a number of locations in the panel and a variety of damage mechanisms that lead to the final collapse and are extremely complex to be understood and reproduced in the numerical analysis.

However, the numerical model well reproduces the mechanism of the local skin buckling, that begins with small waves near the lower edge of the shell and then propagates with bigger waves, centrally located.

7 Conclusions

The results of an experimental and numerical investigation of the buckling and post-buckling behaviour of CFRP stiffened cylindrical shells have been presented.

The collapse of the stiffened shells occurred at a load of about four times the buckling load, confirming the post-buckling strength capabilities of stiffened shells as a significant potential for weight saving.

The collapse was due to the contemporary buckling of 5 stiffeners and was very destructive for the panel.

Work is now in progress to well understand the failure mechanisms leading to the collapse and to set up damage laws in the numerical model so to better predict the real behaviour.

Acknowledgements

This work was supported by the European Commission, Competitive and Sustainable Growth Programme, Contract No. G4RD-CT-1999-00103, project POSICOSS. The information in this document is provided as is and no guarantee or warranty is given that the information is fit for any particular purpose. The user thereof uses the information at its sole risk and liability.

References

- [1] Jullien et al. *Buckling of Shell Structures on Land, in the Sea and in the Air*. Lyon Symposium, Elsevier Applied Science, 1991.
- [2] Simitzes G.J., Shaw D. and Sheinman. Stability of Imperfect Laminated Cylinders: a Comparison between Theory and Experiment. *AIAA Journal*, Vol. 23, No. 7, pp. 1086-1092, 1985.
- [3] Singer J., Arbocz J. and Weller T. *Buckling Experiments: Experimental Methods of Thin-Walled Structures*. Vol. 1, John Wiley & Sons, New York, 1998.
- [4] Bisagni C. Buckling Tests of Carbon-Epoxy Laminated Cylindrical Shells under Axial Compression and Torsion. *XXI ICAS Congress*, Melbourne (Australia), 1998.
- [5] Weller T. and Singer J. Durability of Stiffened Composite Panels under Repeated Buckling. *International Journal of Solids Structures*, Vol. 26, No. 9/10, pp. 1037-1069, 1990.
- [6] Stevens K. A., Ricci R. and Davies G. A. O. Buckling and Postbuckling of Composite Structures. *Composites*, Vol. 26, pp. 189-199, 1995.
- [7] Lilloco M., Butler R., Hunt G. W., Watson A., Kennedy D. and Williams F. W. Optimum Design and Testing of a Post-Buckled Stiffened Panel. *American Institute of Aeronautics and Astronautics*, AIAA-2000-1659, pp. 1-10, 2000.
- [8] Bisagni C. Experimental Buckling of Thin Composite Cylinders in Compression. *AIAA Journal*, Vol. 37, No. 2, pp. 276-278, 1999.
- [9] Bathe KJ. *Finite element procedures in engineering analysis*. Englewood Cliffs, New Jersey: Prentice-Hall Inc., 1982
- [10] Bisagni, C. Numerical Analysis and Experimental Correlation of Composite Shell Buckling and Post-Buckling. *Composites Part B: Engineering*, Vol. 31, No. 8, pp. 655-667, 2000.
- [11] *LS-DYNA Manuals*, Livermore Software Technology Corporation, Version 960, March 2001
- [12] IEPG-CTP-TA 21 guidelines, *Collection of Test Methods and Related Tools*, 1989.